

Supporting Information

Crystallization of Organic Molecules: Nonclassical Mechanism Revealed by Direct Imaging

Authors: Yael Tsarfati^{1†}, Shaked Rosenne^{1†}, Haim Weissman¹, Linda J. W. Shimon⁴, Dvir Gur², Benjamin A. Palmer³, and Boris Rybtchinski^{1*}

[†]These authors contributed equally to this work.

Affiliations:

¹Department of Organic Chemistry, Weizmann Institute of Science, Rehovot, Israel

²Department of Chemical Research Support, Weizmann Institute of Science, Rehovot, Israel

³Departments of Physics of Complex Systems and Molecular Cell Biology, Weizmann Institute of Science, Rehovot, Israel

⁴Department of Structural Biology, Weizmann Institute of Science, Rehovot, Israel

*Correspondence to: boris.rybtchinski@weizmann.ac.il

Table of Contents

| | |
|-----------------------|----|
| Materials and Methods | 1 |
| Figures | 5 |
| References | 40 |

Other Supplementary Materials for this manuscript includes the following:

Crystallographic data for compound **2** are available free of charge from the Cambridge Crystallographic Data Centre under reference CCDC 1583164.

Materials and Methods

Solvents and reagents were purchased from commercial sources and used as received, unless otherwise specified. Organic solvents for spectroscopic studies were of spectroscopic or HPLC grade, dried over molecular sieves (3 Å), and filtered over 0.2 µm PTFE syringe filters prior to use. All procedures with air-sensitive compounds were performed under inert gas atmosphere (dried nitrogen or Argon) using a glovebox (MBRAUN, Labmaster) or standard Schlenk techniques. Organic solvents used for these procedures were degassed with Argon and stored over molecular sieves (3 Å) in the glovebox. Deionized water was purified with a Barnstead NANOpure Diamond water system (18.2 MΩ). No unexpected or unusually high safety hazards were encountered.

Synthesis

Compounds **1** and **2** were synthesized according to literature procedures.¹²

UV-vis and emission spectroscopy

UV-vis absorption measurements were carried out on a Cary-5000 spectrometer (Varian) using quartz cuvettes of 4 or 10 mm light paths. Emission measurements were performed using Cary Eclipse fluorimeter (Varian). For fluorescence measurements, the excitation/emission geometry was 90°.

Transmission electron microscopy (TEM)

TEM samples were prepared by applying 2.4 µl of each sample onto 300-mesh copper grid coated with carbon (on nitrocellulose support) or onto a 300-mesh copper grid coated with holey carbon (Pacific Grid-Tech supplies). The solutions were left to dry

at ambient conditions. Imaging was performed using Tecnai T12 transmission electron microscope operated at 120 kV, equipped with a TVIPS F244HD or OneView CCD digital cameras.

Cryo-TEM

Vitrified samples were prepared by applying 6.5 μl of each sample to a 300-mesh copper grid coated with holey carbon (Pacific Grid-Tech supplies). The samples were blotted at 25°C and 95% relative humidity, and plunged into liquid ethane using Leica EM-GP Automatic Grid Plunger. Specimens were introduced into the microscope using a Gatan 626 cooling holder and transfer station and were equilibrated at -178°C in the microscope prior to the imaging. Imaging was performed using a Tecnai G2 TWIN-F20 microscope equipped with a field emission gun (FEG) operating at 200 kV and a post column Gatan Energy Filter (GIF). Images were recorded using a Gatan US4000 CCD digital camera or a post-GIF Gatan K2 Summit direct detection camera (Gatan Inc.) operated in counting mode or a Tecnai T12 transmission electron microscope operated at 120 kV, equipped with a TVIPS F244HD CCD digital camera.

Single crystals synchrotron x-ray diffraction

Red crystalline needles of **2** precipitated out of water/THF=1/1 (v/v) solution. The samples were coated in Paratone oil and mounted in loops before being flash frozen in liquid nitrogen. X-ray diffraction data were measured at 100K beamline BL13 at the ALBA synchrotron³ with $\lambda=0.80\text{\AA}$. Crystal Data: $\text{C}_{35}\text{H}_{30}\text{N}_2\text{O}_4$, red needle, $0.30 \times 0.50 \times 0.10 \text{ mm}^3$, Monoclinic, $P2_1/c$, $a = 33.863(7) \text{\AA}$, $b = 7.3660(15) \text{\AA}$, $c = 21.085(4) \text{\AA}$, $\beta=100.50(3)^\circ$, $T = 100 \text{ K}$, $V = 5171.2(19) \text{\AA}^3$, $Z = 8$, $F_w = 530.61 \text{ g/mol}$, $D_c = 1.363 \text{ g/cm}^3$. 6552 reflections were collected with MXCube, $R_{\text{merge}} = 0.0845$. Data were

processed with HKL2000 and scaled with Scalepack. Structure was solved by direct methods with SHELXS-14 and refined with SHELXL-13 to a final R factor of 0.0623 for all reflections $I_{\text{sigma}} > 2$ and 0.1033 for all data.

Powder X-ray diffraction (pXRD)

Precipitates were allowed to air dry. Measurements were carried out in reflection mode using a TTRAX III (Rigaku) diffractometer equipped with a scintillation detector and a rotating Cu anode operating at 50 kV and 200 mA in Bragg-Brentano geometry.

Dynamic light scattering (DLS)

The change in hydrodynamic diameter in crystallization of **1** was followed from the initial sample preparation till the dispersion of the value.

The measurements were performed on a Malvern Zetasizer Nano ZSP with a fixed angle of detection (173°). The temperature during DLS measurement was 18°C . A total of 10 measurements were taken for each time point representation (1.6 min for each measurement) every 5 minutes.

Hyper Rayleigh scattering (HRS)⁴

Measurements were made using a 100fs pulsed Ti:Sapphire laser with 80MHz repetition rate (Coherent, Chameleon Ultra II) at 800 nm. The laser was focused using a standard 10X objective into a cuvette containing a solution of crystals. The collection was

done at a 90° with respect to the exciting beam using another standard 10X objective. The signal was imaged into a monochromator (Princeton Instruments, SP2150i) and sent into a photomultiplier detector assembly (PicoQuant, PMA 175). The detector and the laser trigger output were connected to a time-correlated single-photon counting system (Picoquant HydraHarp 400).

Figures

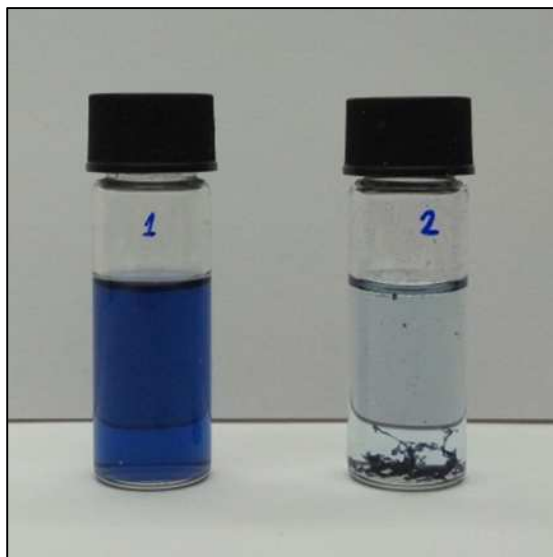


Figure S1. A photograph of **1** in 10^{-4} M water/THF=85/15 (v/v) solution in 4 ml vials: Left: Immediately after preparation, the solution is clear blue. Right: 3 weeks aged solution, nearly complete precipitation.

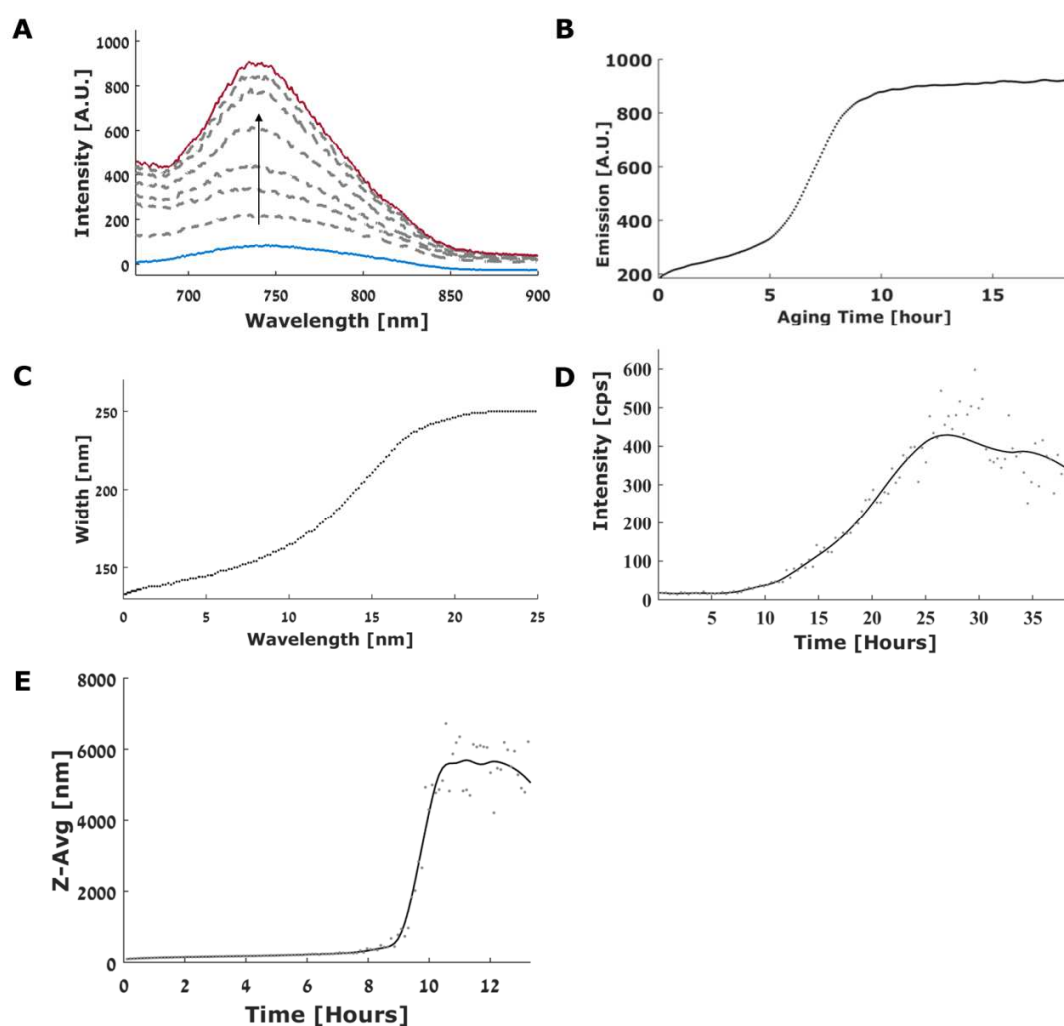


Figure S2. Crystallization of **1** in 10^{-4} M water/THF=85/15 (v/v) solution. Kinetics from various spectroscopic methods: **(A)** Emission follow-up of crystallization of **1**: 0 h (Blue), 21 h (red), 1h, 5h, 6h, 7h, 8h, 9h (bottom to top in gray). **(B)** Emission intensity at 740 nm (the maximum) over time, derived from the full measurement depicted in **(A)**. **(C)** Broadening (change of width) of the dominant absorption band (470-800 nm) over time. **(D)** HRS signal of the sample at 400 nm monitored over time. Excitation at 800 nm, detection at 394-405 nm. **(E)** Hydrodynamic radius (from DLS) over time. All kinetic curves show sigmoidal behavior, with small deviations arising from measurement limitations.

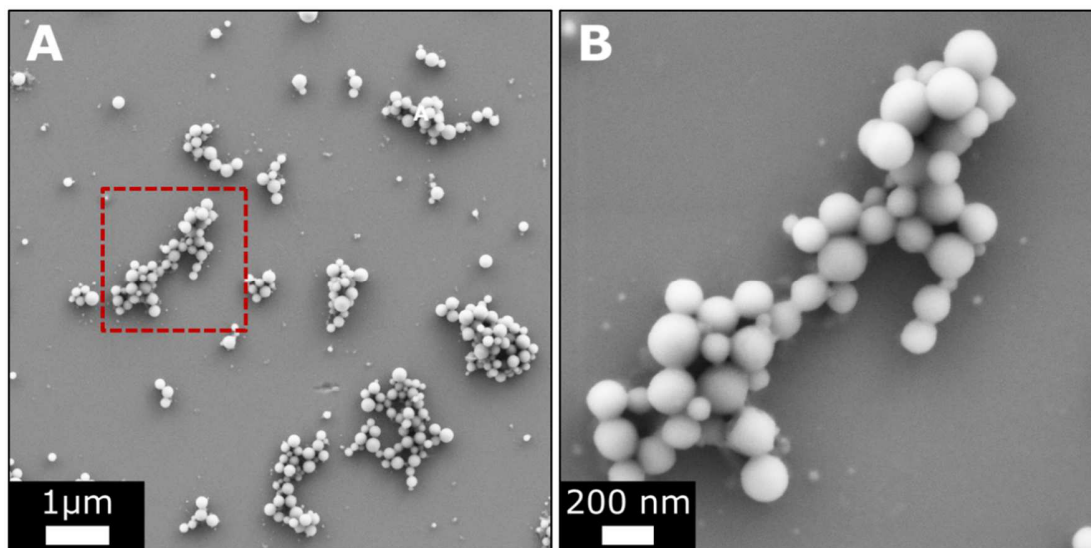


Figure S3. (A) SEM images of dried solution of **1** in water/THF=85/15 (v/v), 10^{-4} M, immediately after preparation. (B) Magnified view of the marked area in A.

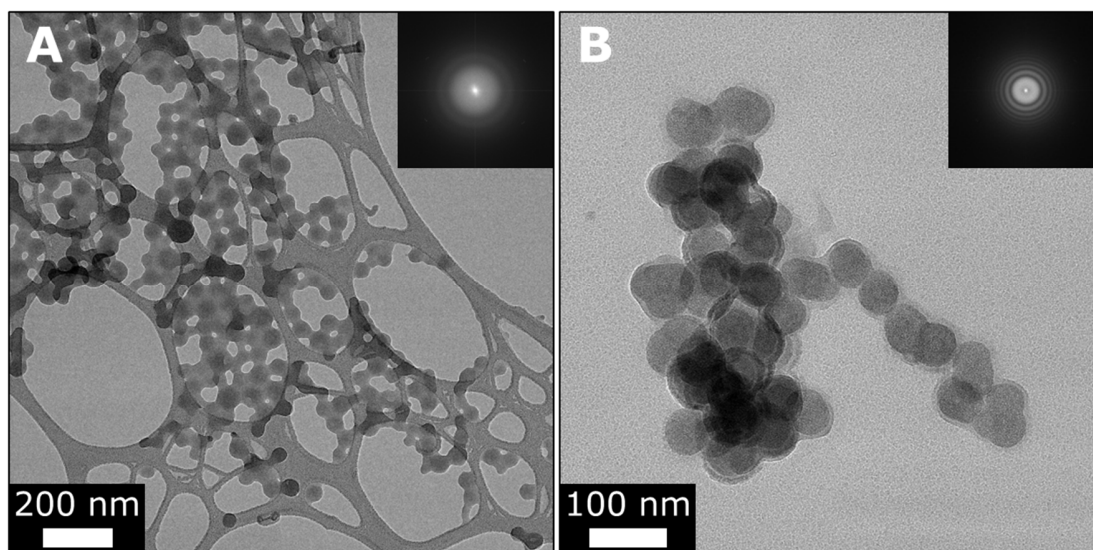


Figure S4. (A) TEM images of dried solution of 1 in water/THF=85/15 (v/v), 10^{-4} M, immediately after preparation. Clusters of spherical aggregates are detected. (B) Magnified view of such cluster.

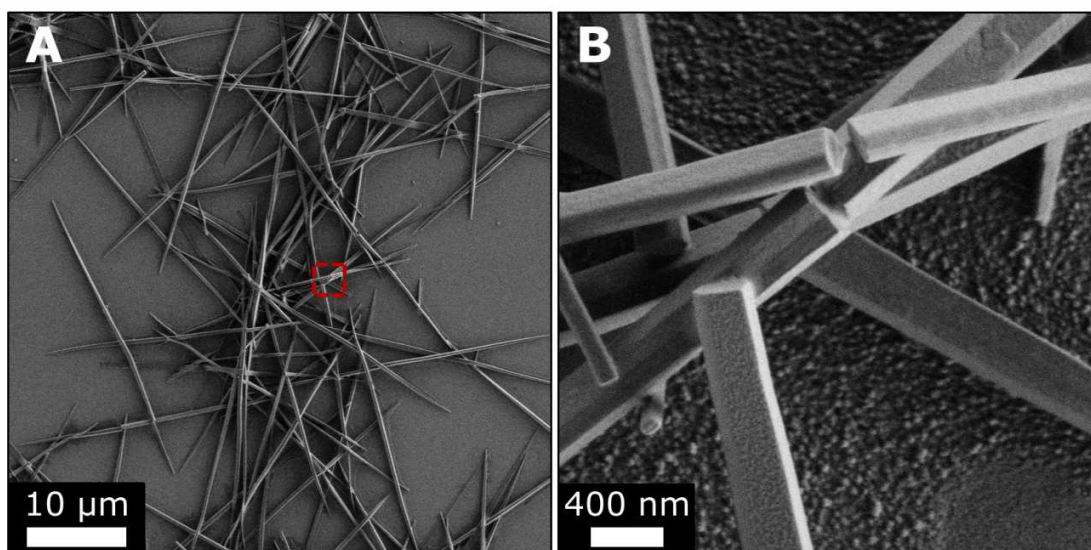


Figure S5. SEM images of dried solution of **1** in water/THF=85/15 (v/v), 10^{-4} M, after 2 months aging. **(A)** Elongated crystals. **(B)** Magnified view of the marked area in **A** showing faceted crystals.

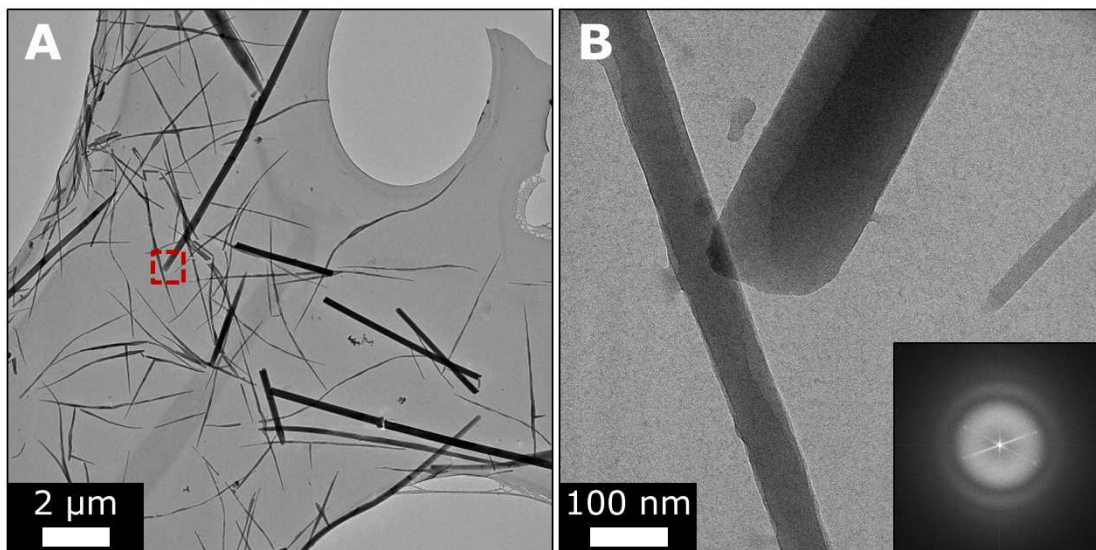


Figure S6. TEM images of dried solution of **1** in water/THF=85/15 (v/v), 10^{-4} M, after 24 h aging. **(A)** Elongated crystals are detected. **(B)** A magnified view of a representative crystal (marked in **A**). Inset: FFT of the image indicating 1.6 nm periodicity.

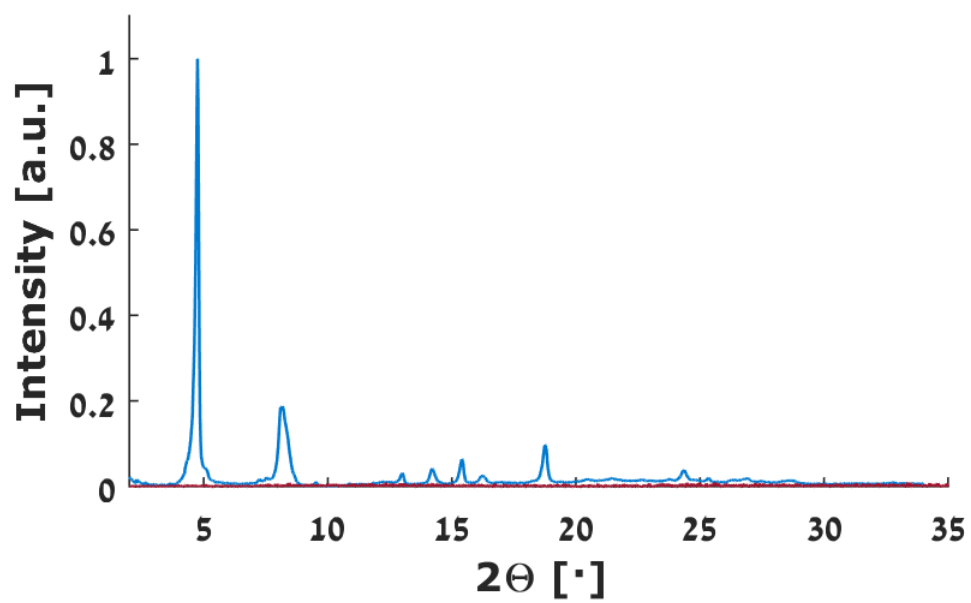


Figure S7. pXRD of dried solution of **1** in water/THF=85/15 (v/v), 10^{-4} M: dried immediately after preparation (red), and after one week aging (blue).

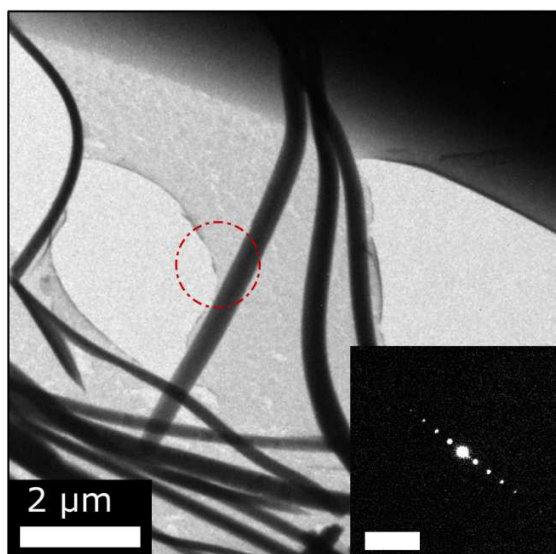


Figure S8. An example of electron diffraction pattern, collected from a crystal of compound **1**, from a 24 h age dried sample of **1**: circled is the area from which diffraction was collected. Inset: the corresponding diffraction (reflections: 1.6 nm, 0.8 nm , 0.5 nm and 0.4 nm) . Scale bar is 2 nm⁻¹.

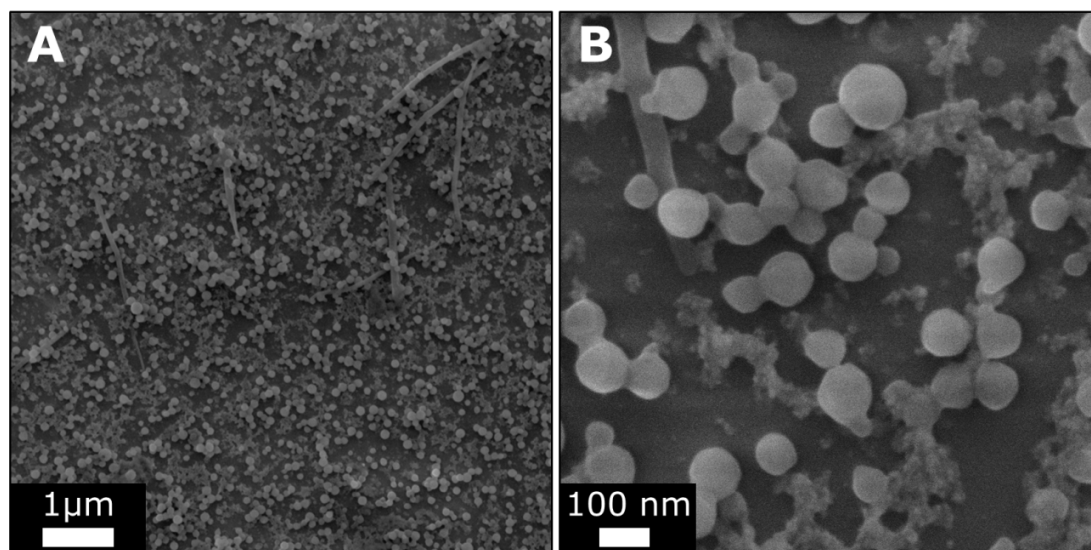


Figure S9. SEM images of dried solution of **1** in water/THF=85/15 (v/v), 10^{-4} M, after 5 h of aging. **(A)** Spherical aggregates and a few crystals. **(B)** Magnified view displaying the spherical aggregates and part of a crystal (top left).

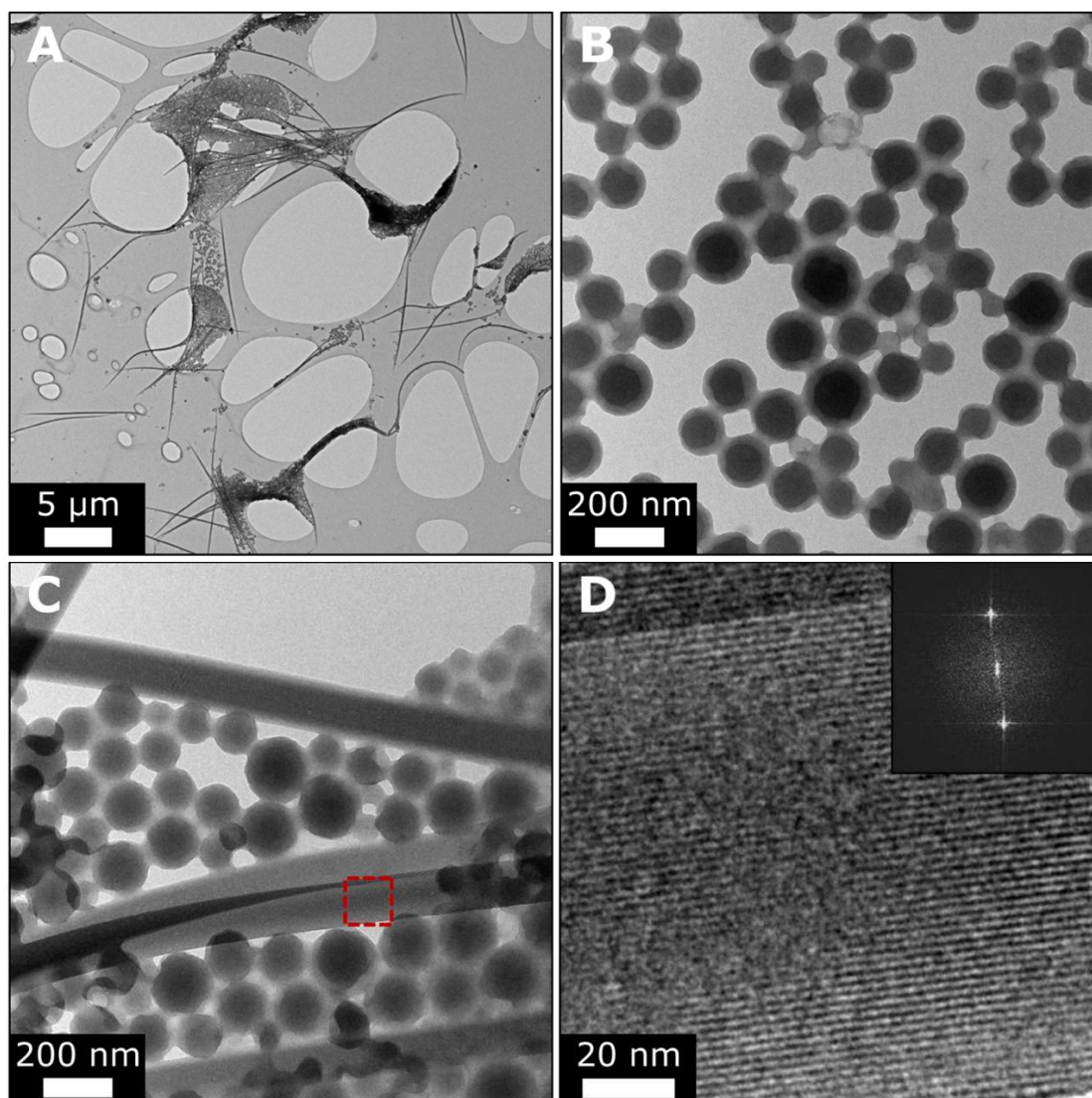


Figure S10. TEM images of dried solution of **1** in water/THF=85/15 (v/v), 10^{-4} M, after 5 h of aging. **(A)** Spherical aggregates and a few crystals. **(B)** Magnified view showing connected round aggregates. **(C)** Magnified view of spheres and crystals. **(D)** Magnified view of the marked area in C. Inset: FFT indicating 2 nm periodicity.

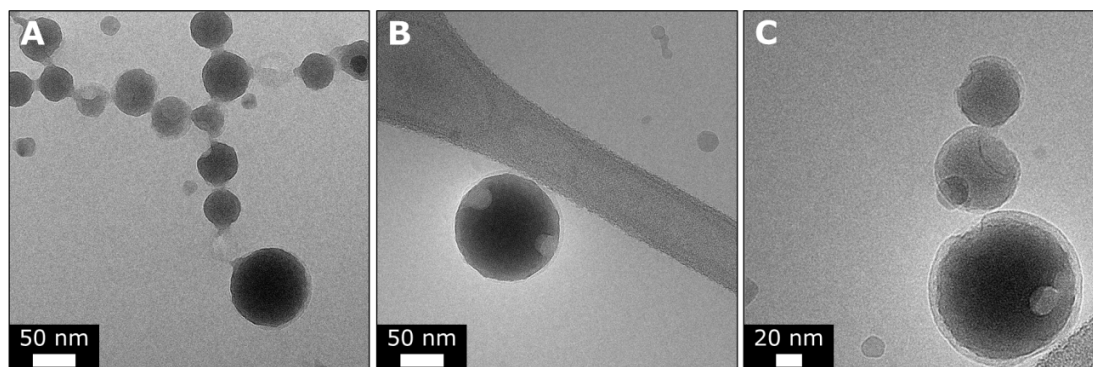


Figure S11. Cryo TEM images of solution of **1** in water/THF=85/15 (v/v), 10^{-4} M, immediately after preparation. Spherical aggregates formed immediately after sample preparation. **(A)** Proximity and connectivity of spheres. **(B)** Isolated sphere. **(C)** Higher magnification of spherical aggregates displays the spherical morphology is not perfect; dents can be found. Moreover, the spheres display two clear phases by contrast, where the inner phase is denser than the outer phase.

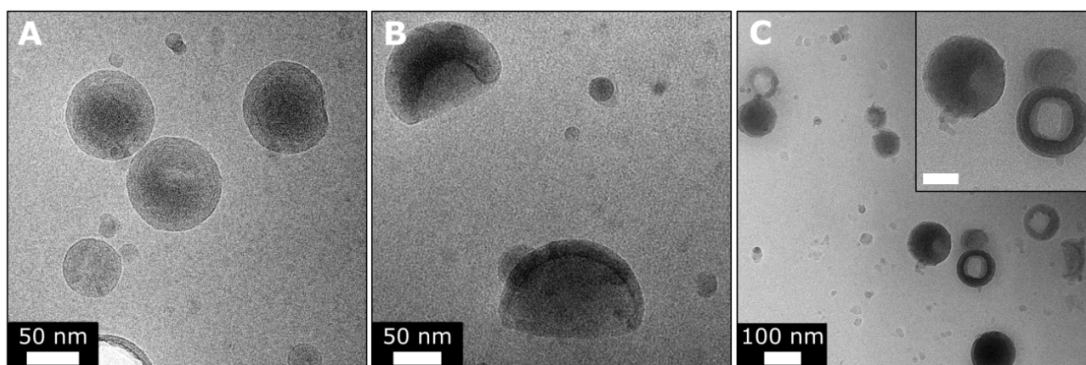


Figure S12. Cryo TEM images of solution of **1** in water/THF=85/15 (v/v), 10^{-4} M, after 45 min aging. **(A)** Spheres displaying a formed higher-contrast (denser) phase. **(B)-(C)** Deformations of the spheres accompanied by higher contrast (denser) phase in the outer part. **(C)** Inset: Magnified view of **C**. Scale bar is 50 nm.

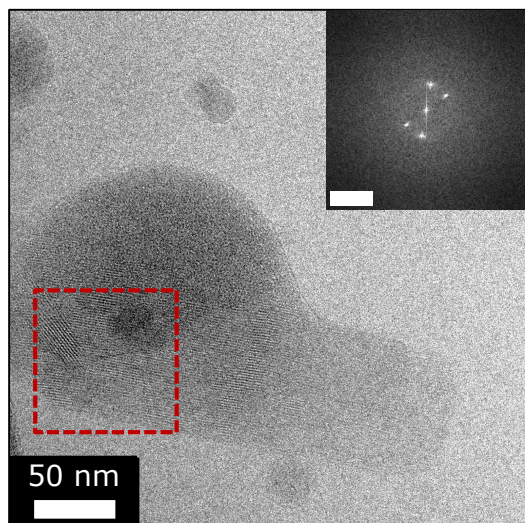


Figure S13. Cryo TEM image of solution of **1** in water/THF=85/15 (v/v), 10^{-4} M, after 30 min aging, showing intermediates connecting the spheres to the crystals. Inset: FFT of the marked area revealing 1.6-1.7 nm periodicity. scale bar 1 nm^{-1} .

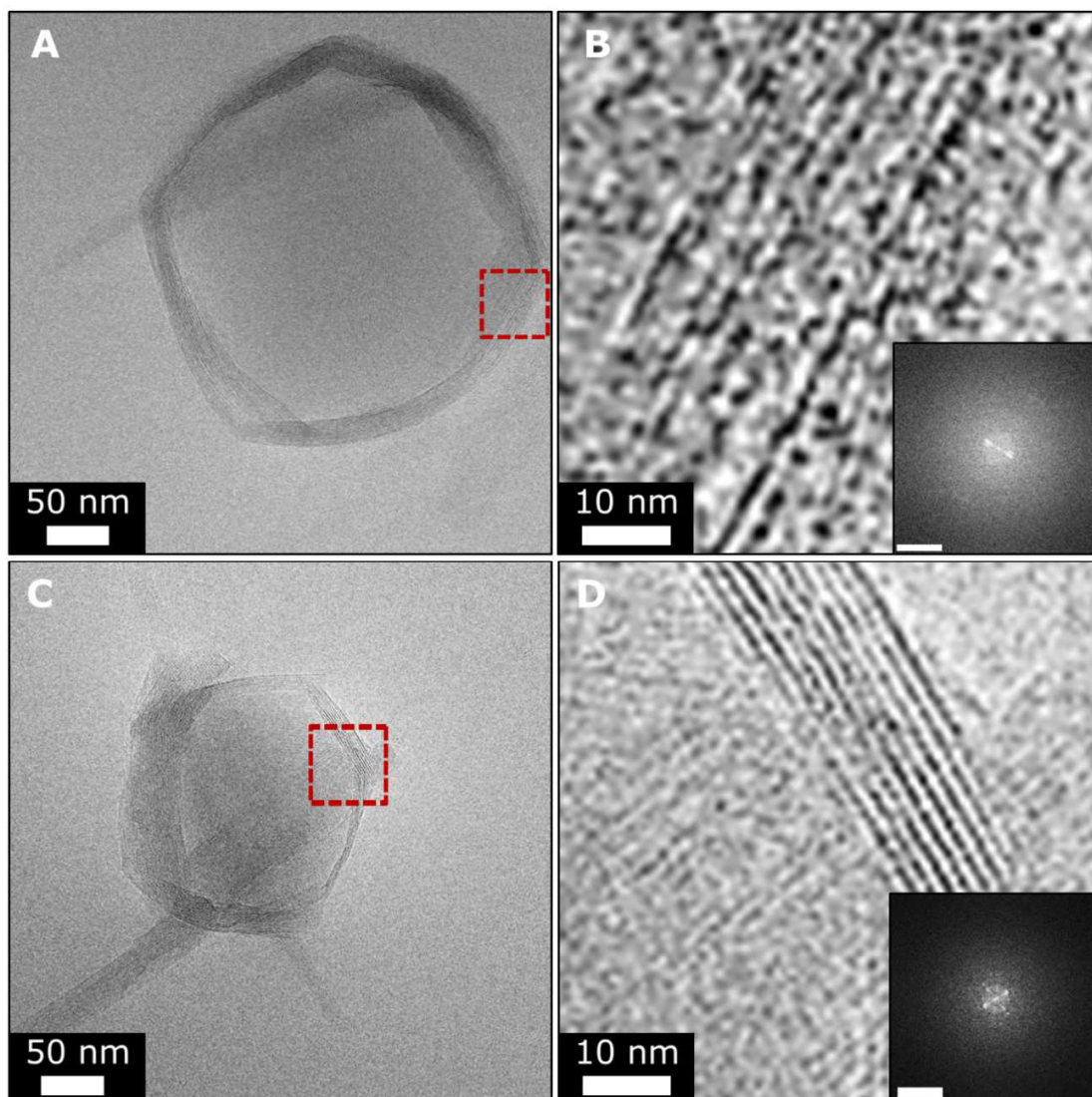


Figure S14. Cryo TEM images of solution of **1** in water/THF=85/15 (v/v), 10^{-4} M, after 45 min aging. **(A)** and **(C)** display examples of spherical aggregates where the outer denser phase develops faceting and emerging lattice fringes. **(B)** and **(D)** are magnified views of the marked areas in **A** and **C** correspondingly. Insets: FFTs reveal periodicities of 1.7 nm for **B** and 1.7 nm and 1.2 nm for **D**. scale bar 2 nm^{-1} .

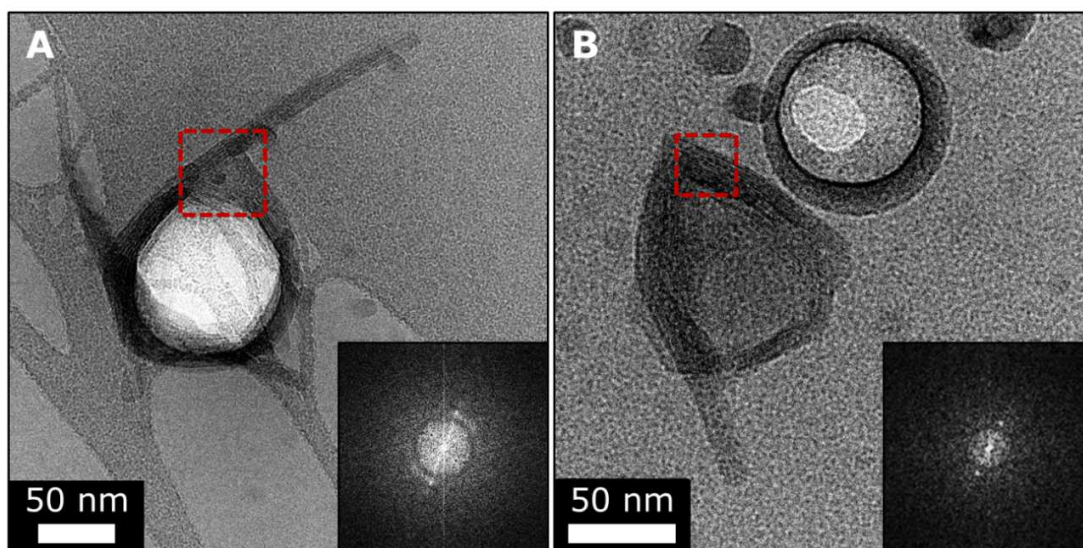


Figure S15. Cryo TEM images of solution of **1** in water/THF=85/15 (v/v), 10^{-4} M, after 50-min aging presenting intermediates connecting the spheres to the crystals. **(A)** Spherical core morphology is apparent and crystals emerge from the outer higher contrast (denser) region. **(B)** Aggregates featuring remnants of spherical cores broken by the faceting in the outer denser region. Insets: FFT of the marked areas reveal periodicity of 1.2 nm (in **A**) and 1.7 nm (in **B**).

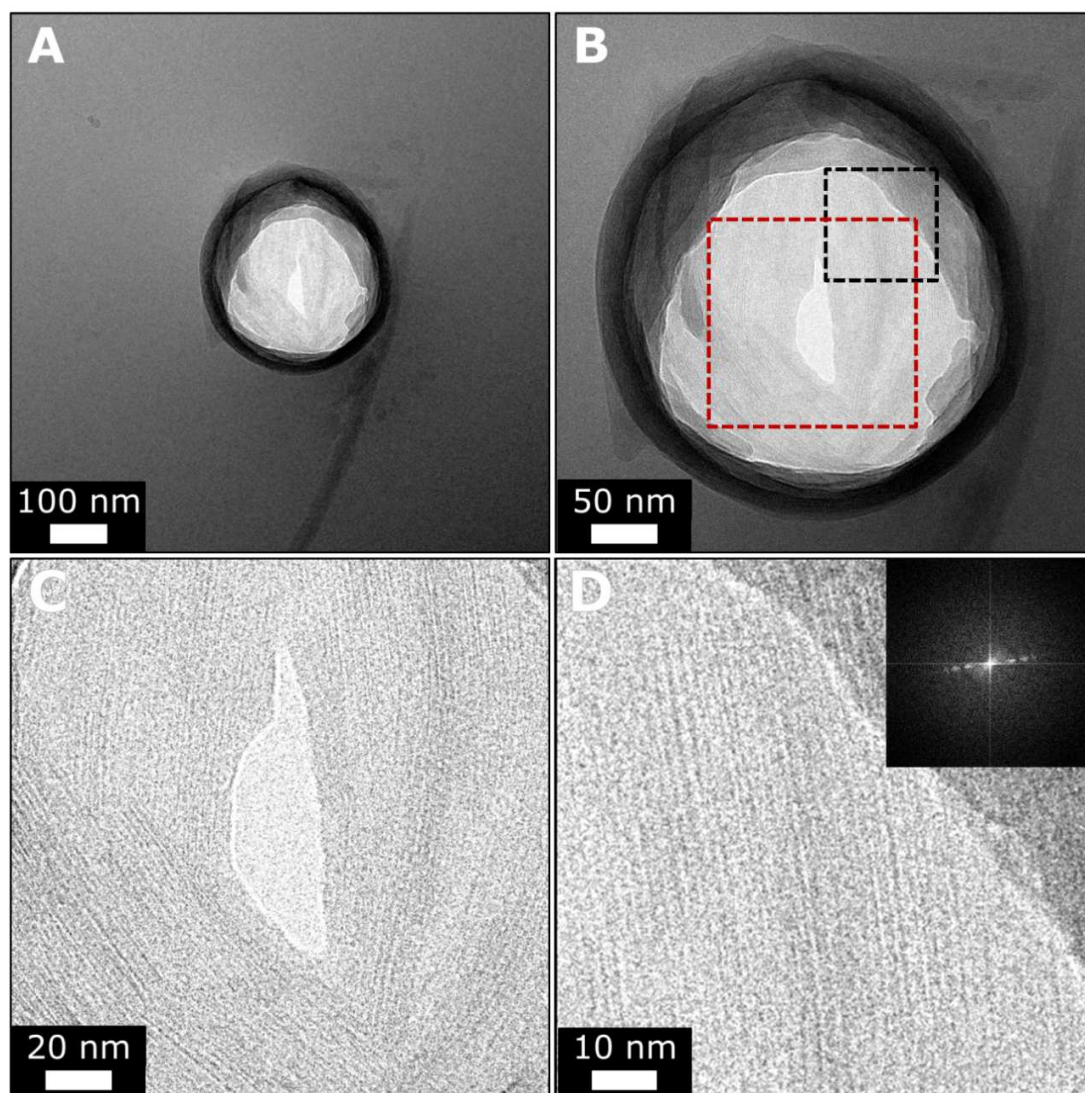


Figure S16. Cryo TEM images of solution of **1** in water/THF=85/15 (v/v), 10^{-4} M, after 4.5 h aging. **(A)** A round aggregate. **(B)** Magnified view of (A). **(C)** Magnified view of the red marked area in **B** showing early lattice fringes. **(D)** Magnified view of the black marked area in **B**, showing lattice fringes which reveal periodicity of 1.3 nm, 1.0 nm, and 2.0 nm as indicated by the FFT (inset).

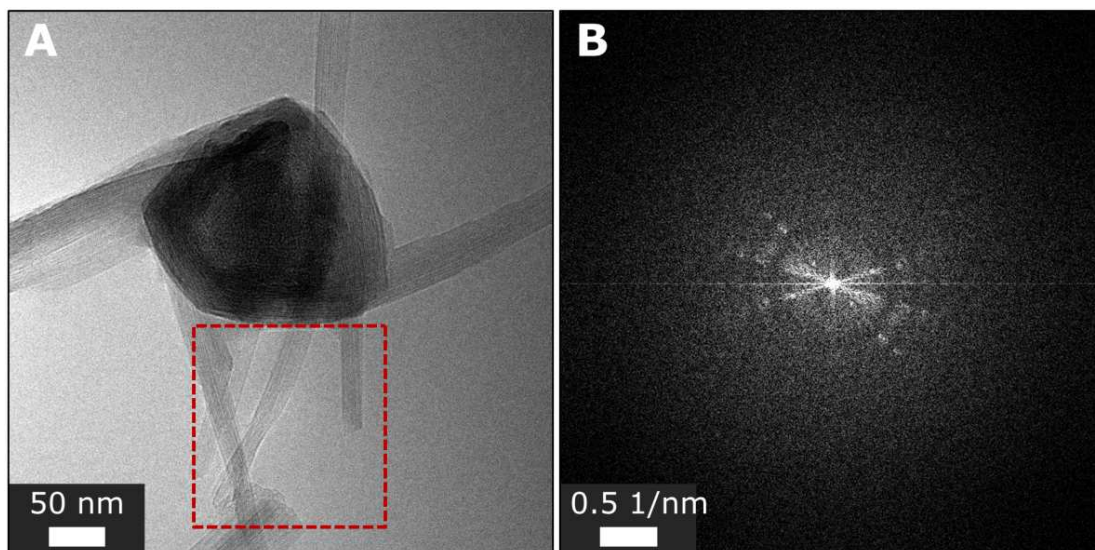


Figure S17. (A) Cryo TEM image of solution of 1 in water/THF=85/15 (v/v), 10^{-4} M, after 4.5 h aging; (B) FFT of the marked area in A revealing periodicities of 4.2 nm, 1.6 nm, 1.5 nm, 1.7 nm and 1.2 nm.

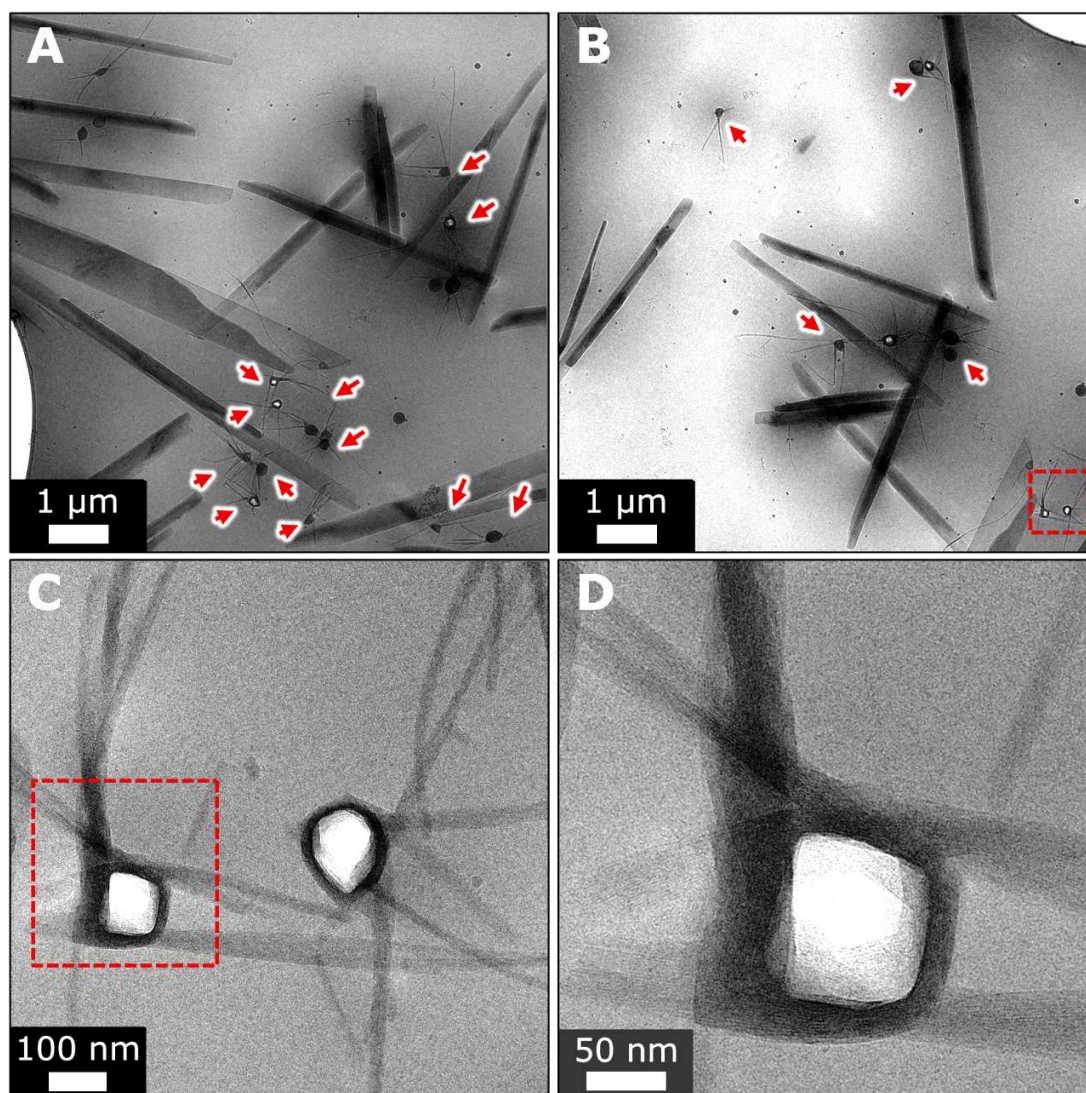


Figure S18. Cryo TEM images of solution of **1** in water/THF=85/15 (v/v), 10^{-4} M, after 4.5 h aging **(A)-(B)** Intermediates surrounded by growing fiber-like crystals are marked by arrows. **(C)** Magnified view of the marked areas in **B**. **(D)** Magnified view of the marked area in **C**. Periodicity of 1.7 nm and 0.9 nm can be detected by FFT.

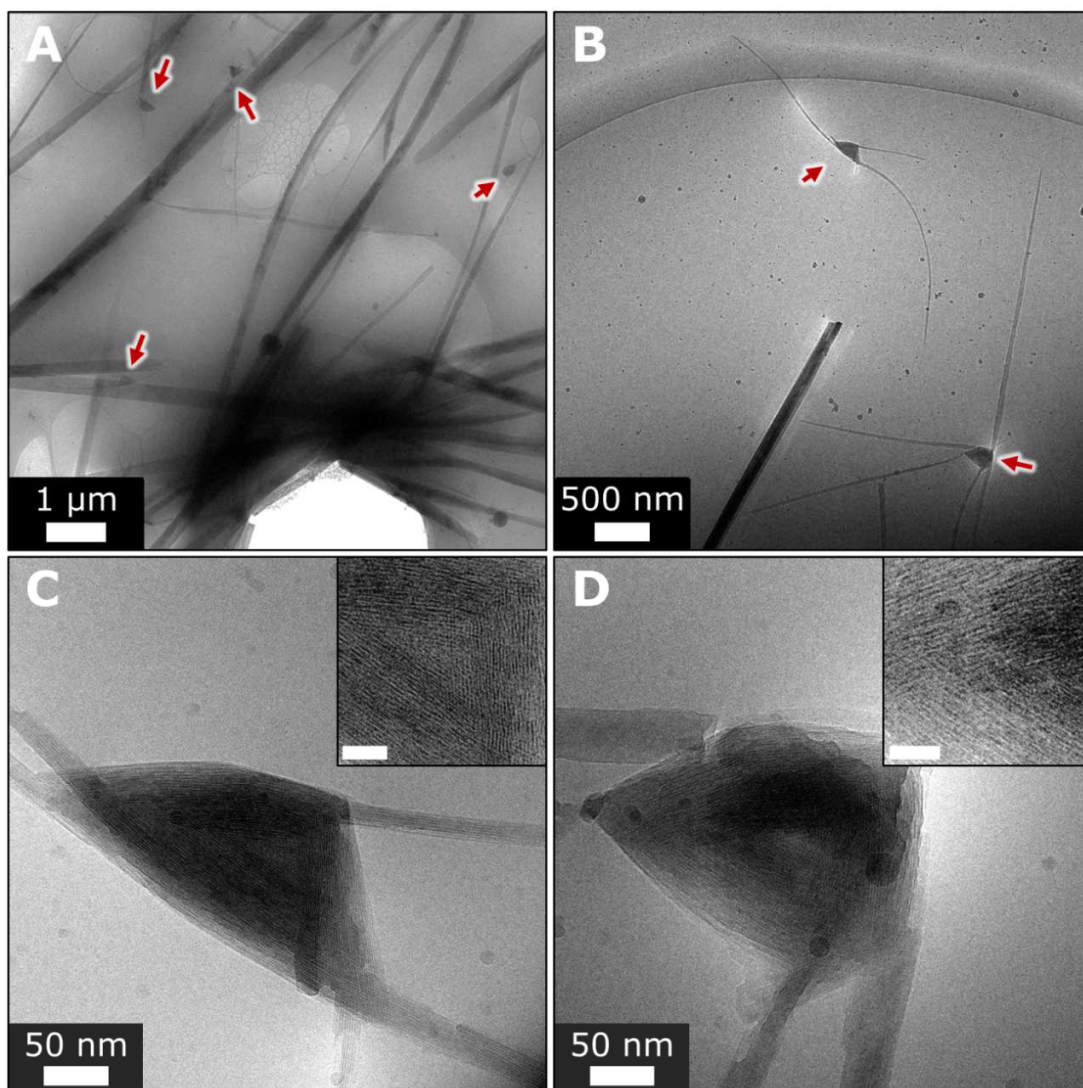


Figure S19. Cryo TEM images of solution of **1** in water/THF=85/15 (v/v), 10^{-4} M, after 7.5-h aging. **(A)-(B)** Elongated crystals, yet some intermediates are still detected, marked by arrows. **(C)-(D)** Magnified view of the intermediates apparent in **B**. Insets: Magnified view of the core regions of the aggregates showing lattice fringes, which reveal periodicities of 2.4 nm, 1.9nm , 1.1 nm for **C** and 0.9 nm, 1.5 nm and 2.2 nm for **D**. Scale bars of insets are 20 nm.

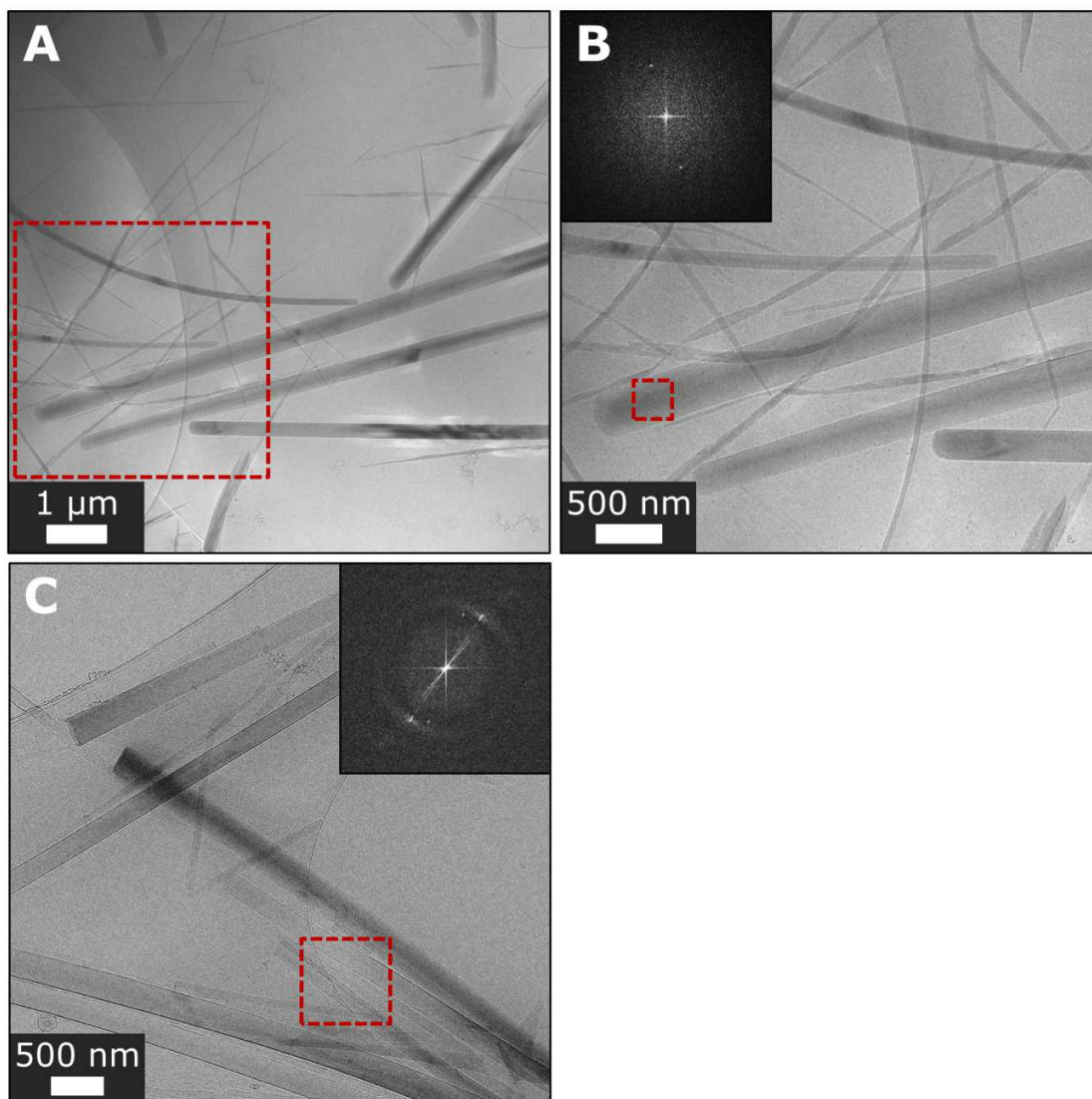


Figure S20. (A) Cryo TEM image of solution of 1 in water/THF=85/15 (v/v), 10^{-4} M, after 24 h aging. (B) A magnified view of the marked area in A, showing a representative crystal. Inset: FFT of the marked area in B revealing 1.4 nm periodicity. (C) Additional representative crystal. Inset: FFT of the marked region in C revealing 1.9 nm, 1.8 nm and 1.7 nm periodicities.

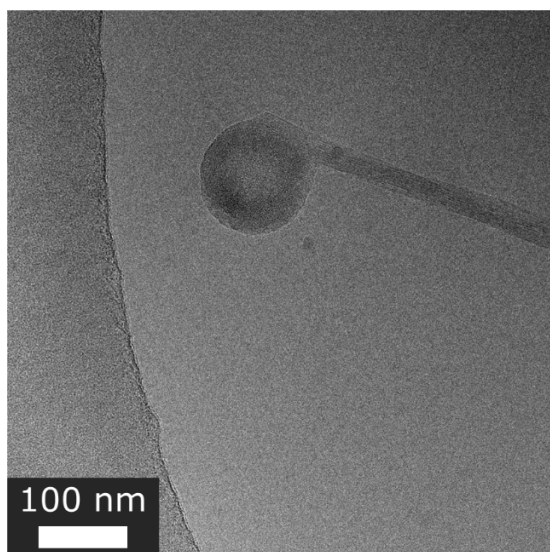


Figure S21. Cryo TEM image of solution of **1** in water/THF=85/15 (v/v), 10^{-4} M, after 4 h aging displaying fusion of spherical aggregate with a crystal.

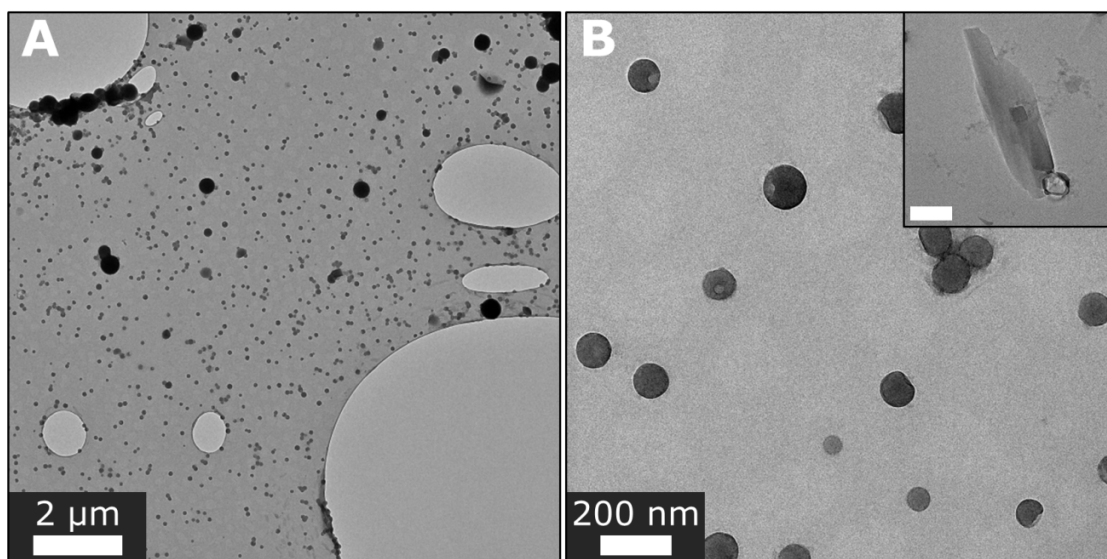


Figure S22. TEM images of dried solution of **1** in water/THF=7/3 (v/v), 10^{-4} M, after 5-day aging. **(A)** Spherical aggregates. **(B)** Magnified view of the aggregates. Inset: an example of detected crystal. Scale bar is 200 nm.

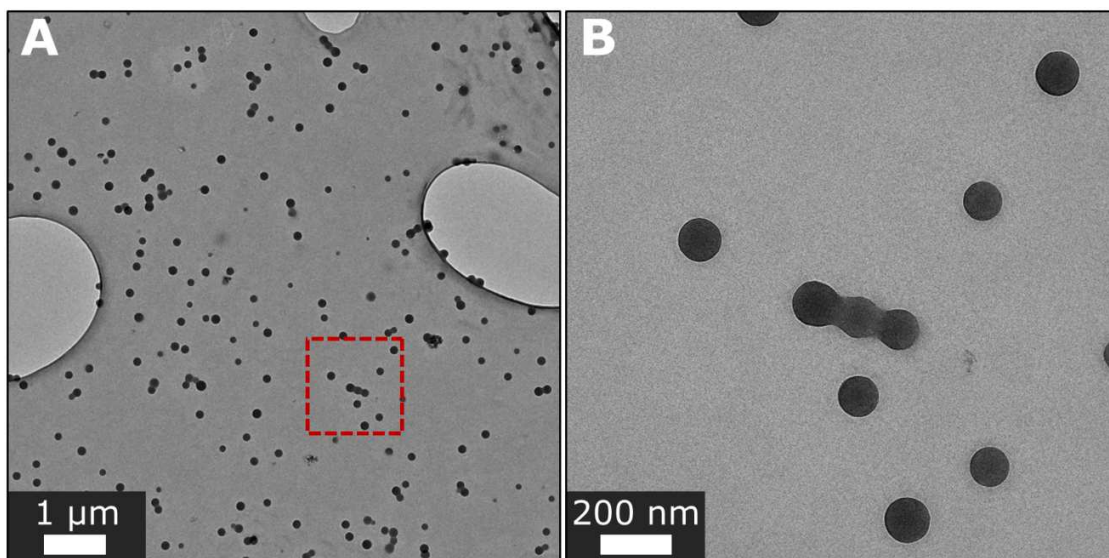


Figure S23. TEM images of dried solution of **1** in water/THF=1/1 (v/v), 10^{-4} M, after 1-year aging. **(A)** Round aggregates are detected. **(B)** Magnified view of the marked area in **A**.

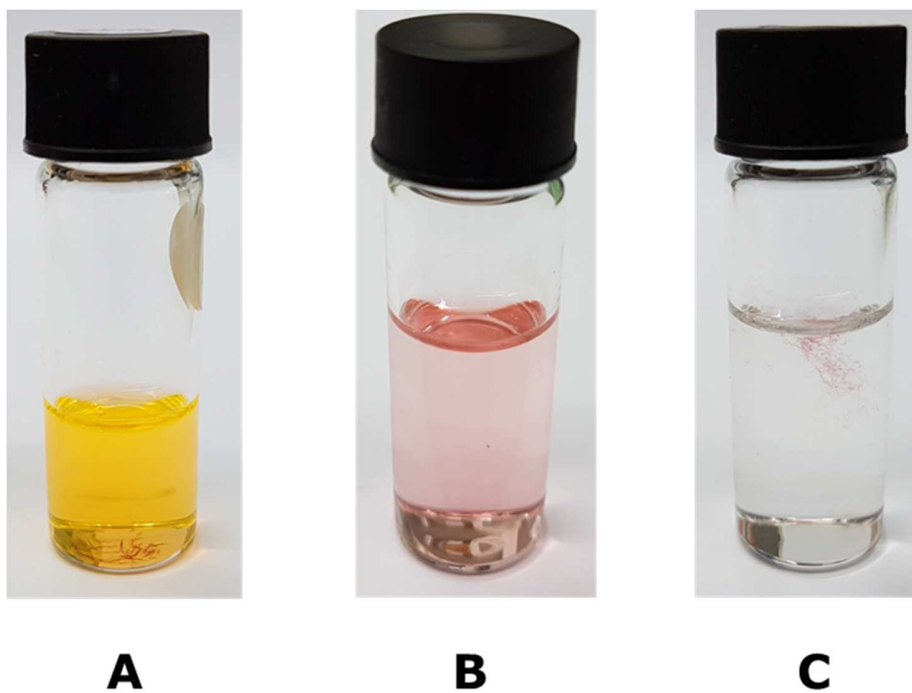


Figure S24. Photographs of **2** in water/THF solutions in 4 ml vials. **(A)** **2** in water/THF=1/1 (v/v), 10^{-4} M, small amount of precipitate is seen at the bottom of the vial. **(B)** **2** in water/THF=3/7 (v/v), 10^{-5} M upon preparation. **(C)** The solution in **B** after 72 hours aging.

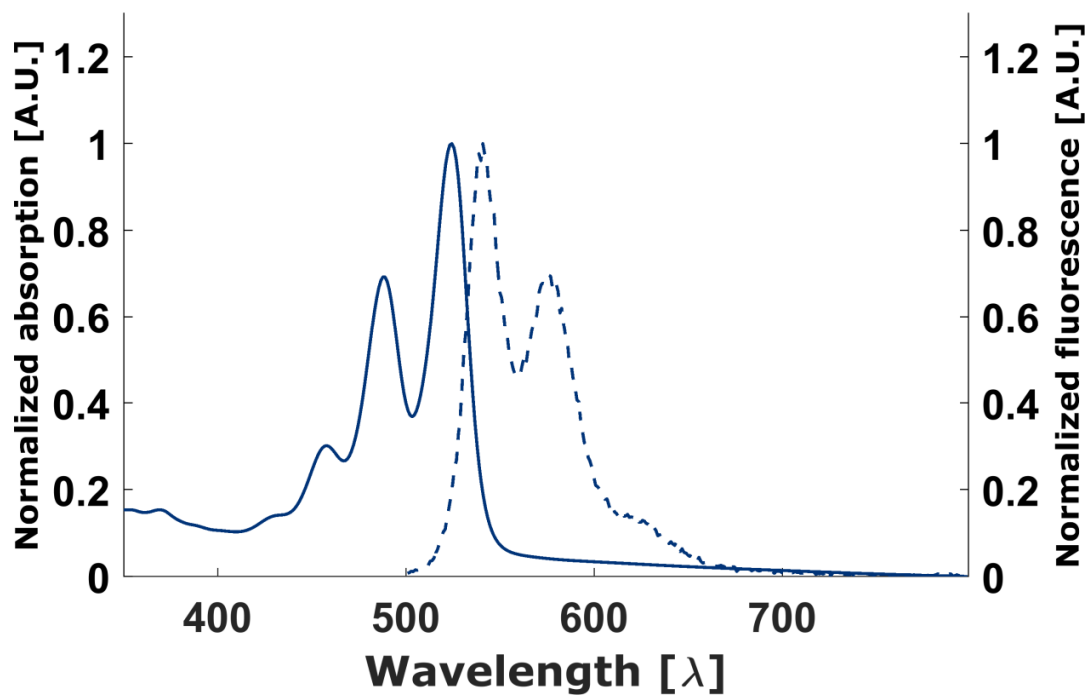


Figure S25. UV-vis and emission spectra of **2** in water/THF=1/1 (v/v), 10^{-4} M.

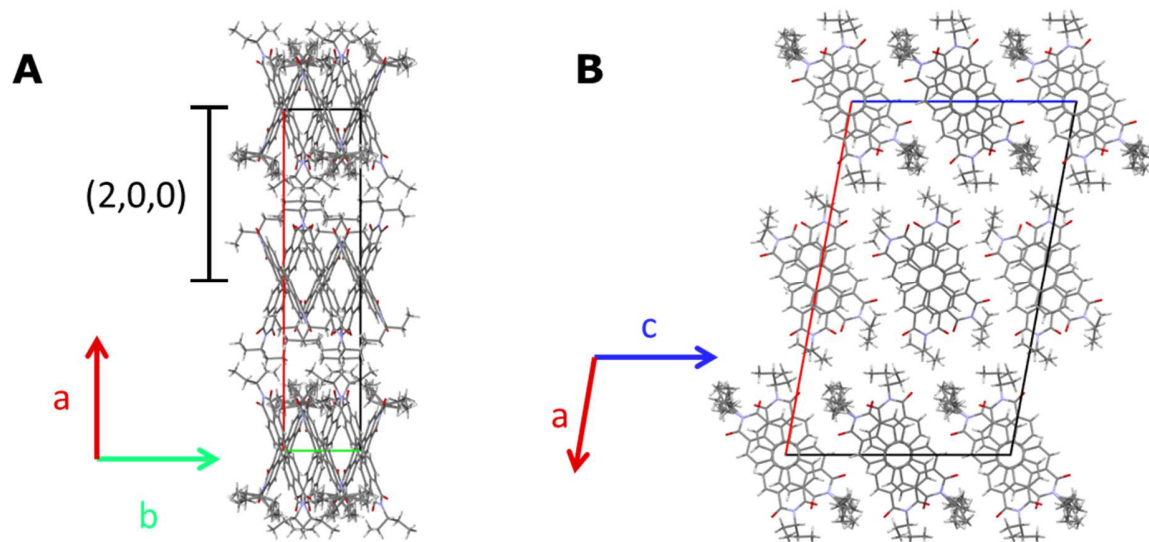


Figure S26. Crystal structure of **2** featuring extended columnar stacks along the b axis. **(A)** View down the c axis showing the (200) spacing of 1.6 nm. **(B)** View down the b axis.

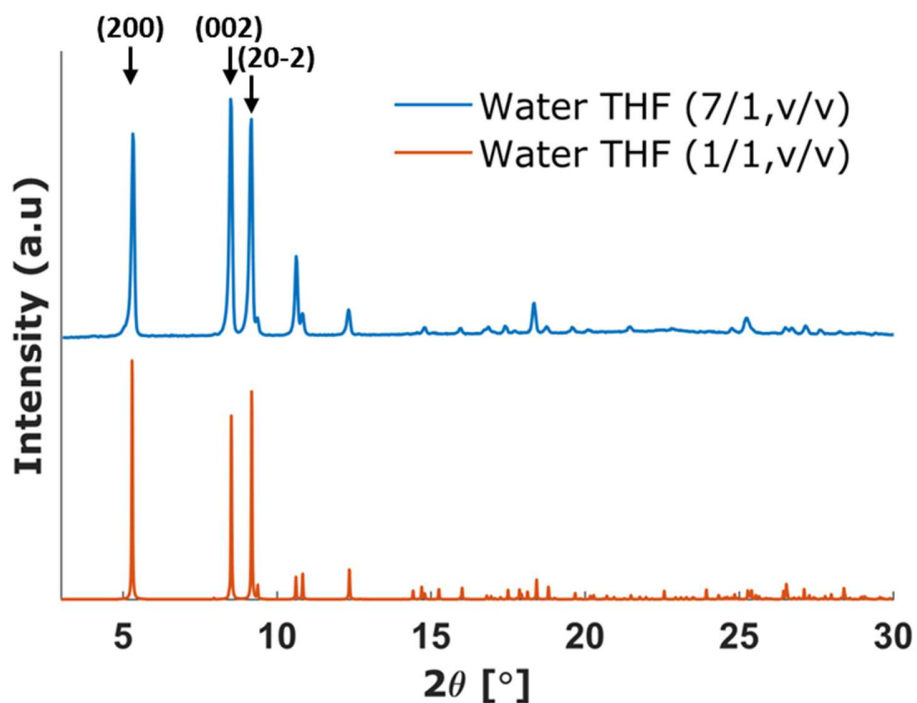


Figure S27. pXRD of precipitate of **2** from water/THF mixtures. Measured diffractogram of **2** precipitated out of water/THF=7/3 (v/v) mixture, 10⁻⁵M (Top). Calculated diffractogram of the single crystal isolated from the water/THF=1/1 (v/v) mixture, 10⁻⁴M (bottom). The measured reflections fit the calculated spectrum. Intensity differences originate from the existence of preferred orientation in the needles and specific measurement geometry, importantly, all measured peaks are accounted for in the simulated spectrum. The (200), (002) and (20-2) indices have spacings of 1.63, 1.033 and 9.69 nm respectively. The calculation of the diffraction pattern was done using Mercury software⁵.

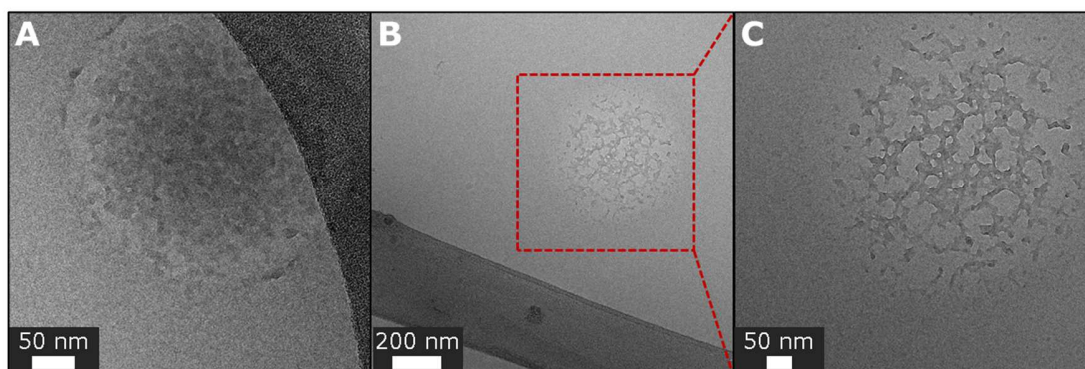


Figure S28. (A)-(B) Amorphous liquid-like prenucleation aggregates of 2 in water/THF=1/1 (v/v), 10^{-4} M. (C) Magnified view of the marked region in B.

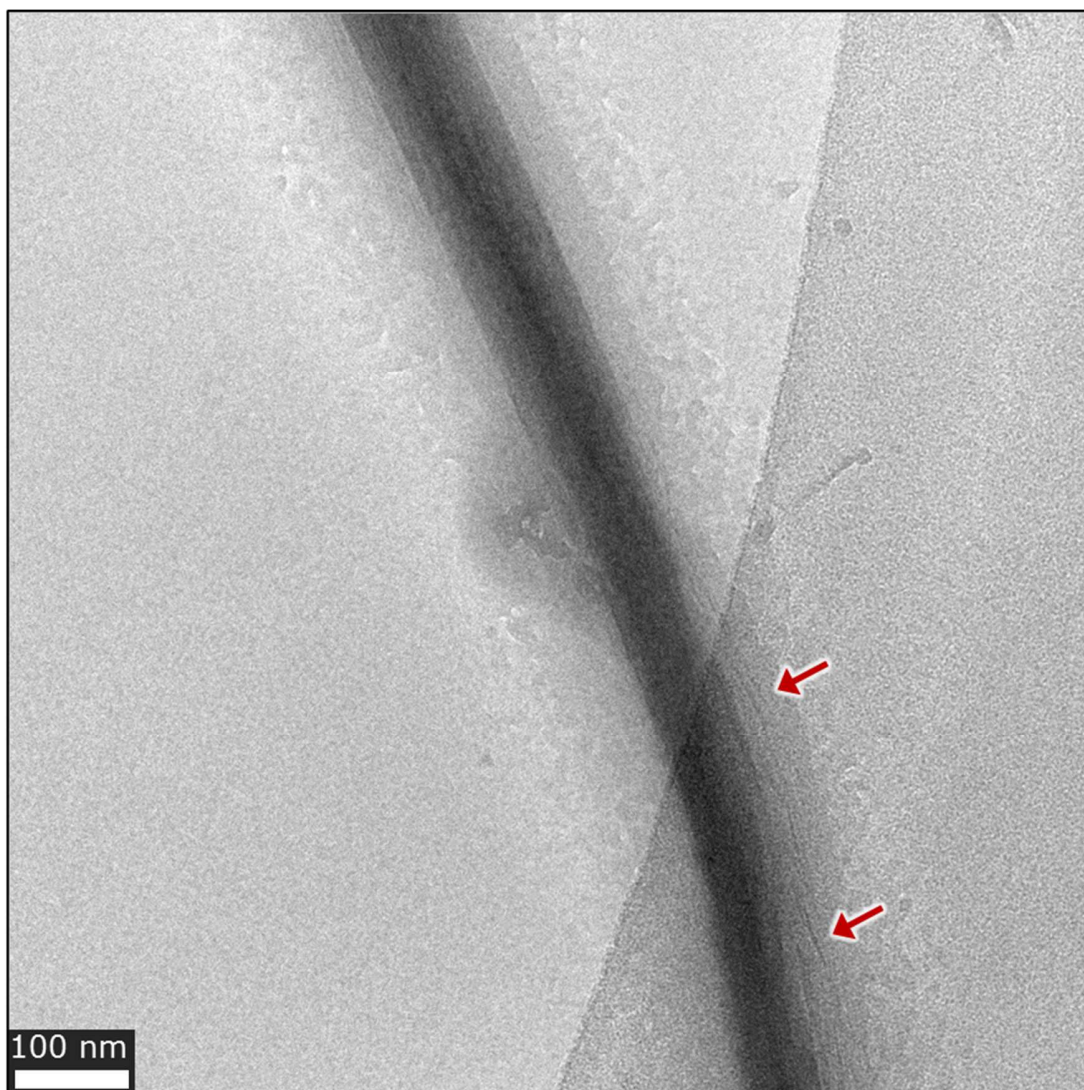


Figure S29. Compound **2** in water/THF=1/1 (v/v), 10^{-4} M. Partly ordered needle is shrouded in an amorphous phase. Arrows point to constituting fibers.

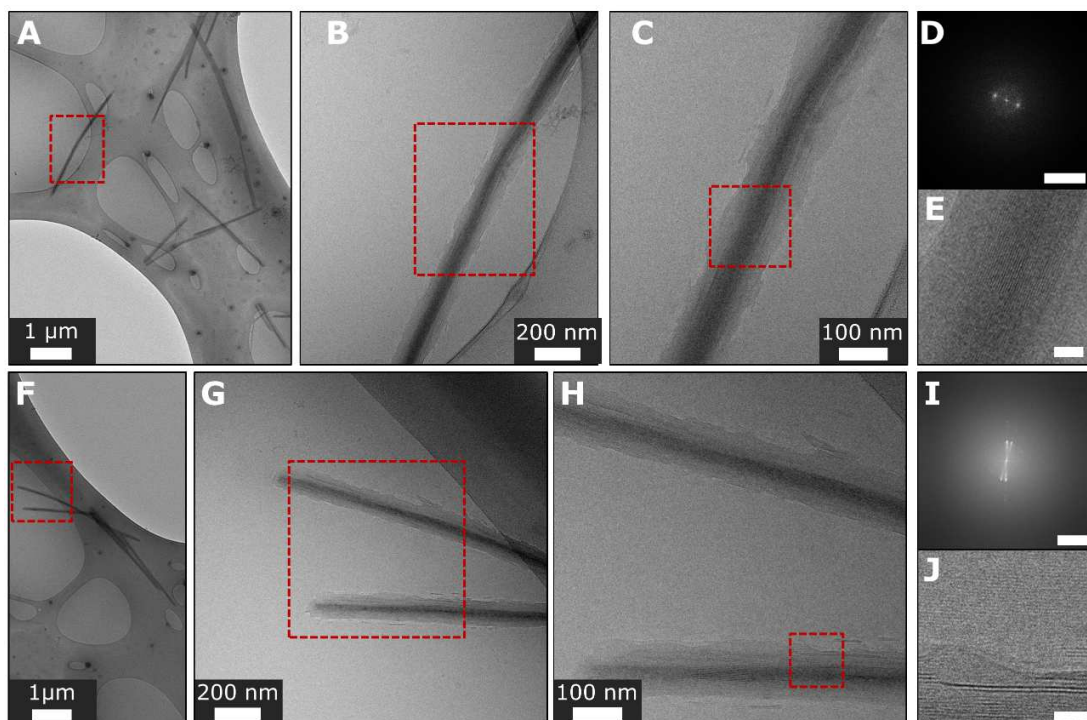


Figure S30. Cryo-TEM images of **2** in water/THF=1/1 (v/v), 10^{-4} M. **(A)** Partly ordered needle shrouded in an amorphous phase. **(B)** Magnified view of the marked region in **A**. **(C)** Magnified view of the marked region in **B**. **(D)** FFT analysis of the region marked in **C** showing 1.6 nm periodicity. Scale bar is 1 nm^{-1} . **(E)** Magnified view of the region marked in **C**, showing apparent lattice fringes. Scale bar is 20 nm. **(F)** Partly ordered adjacent needles shrouded in an amorphous phase. **(G)** Magnified view of the marked region in **F**. **(H)** Magnified view of the marked region in **G**. **(I)** FFT analysis of the region marked in **H** showing 1.6 nm periodicity. Scale bar is 1 nm^{-1} . **(J)** Magnified view of the region marked in **H**, showing apparent lattice fringes. Scale bar is 20 nm.

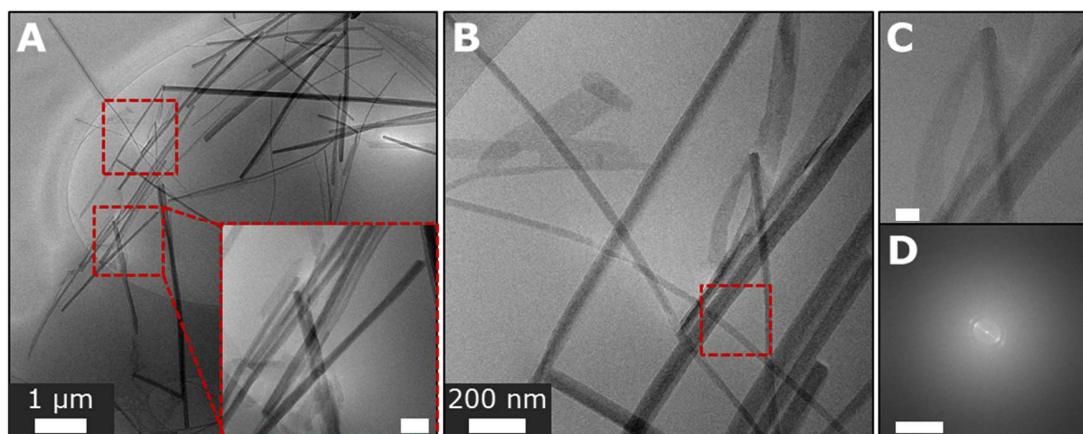


Figure S31. Cryo-TEM images of **2** grown in water/THF=1/1 (v/v), 10^{-4} M. **(A)** Mature needles exhibiting sharp facets. Inset: magnified view of the marked region. Scale bar is 200 nm. **(B)** Magnified view of the marked region in **A**. **(C)** Magnified view of the marked region in **B**. Scale bar is 50 nm. **(D)** FFT of **C** showing spacing periodicities of 1.7 and 1.2 nm.

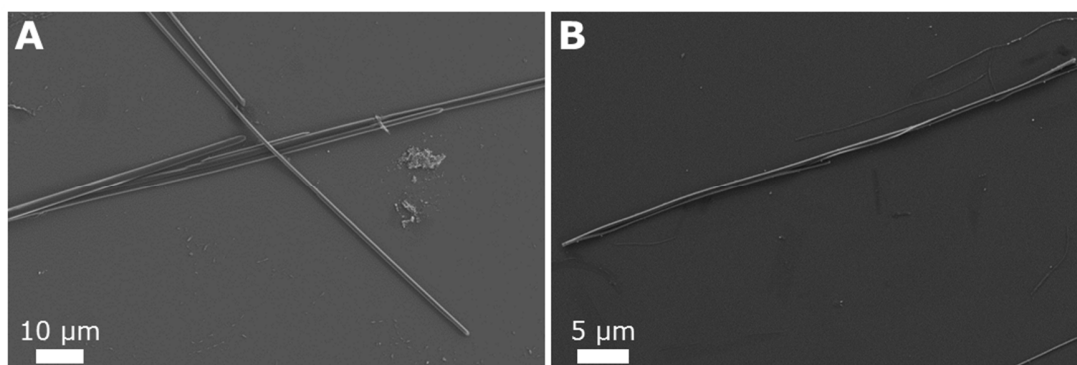


Figure S32. SEM image of needles precipitated out of solutions of **2**. **(A)** From water/THF=1/1 (v/v), 10^{-4} M. **(B)** From water/THF=7/3 (v/v), 10^{-5} M. Crystals grown at low concentration tend to be of smaller sizes.

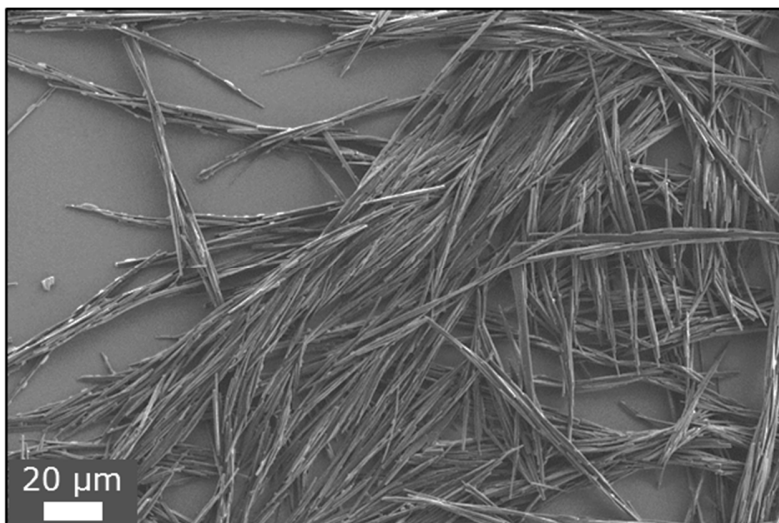


Figure S33. SEM image of needles precipitated out of a solution of **2** in water/THF=7/3 (v/v), 10^{-5} M.

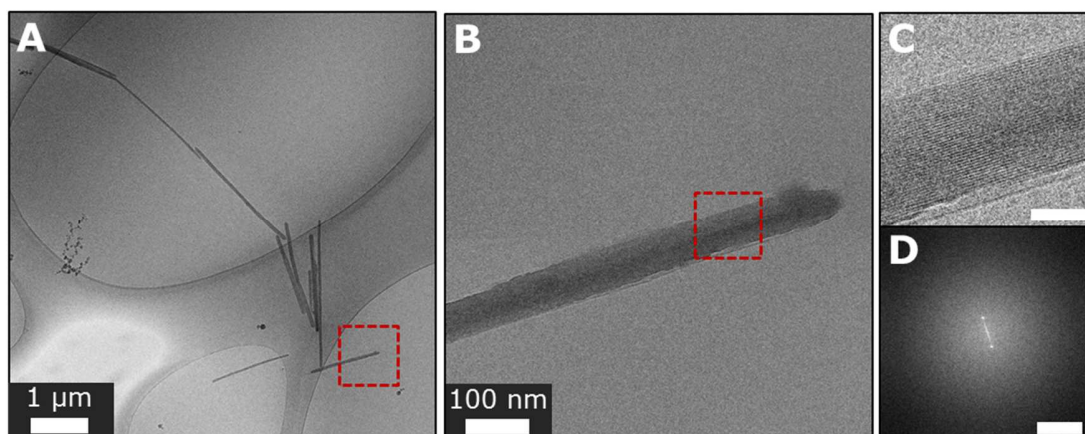


Figure S34. Cryo-TEM images of **2** grown in water/THF=7/3 (v/v) solution, 10^{-5} M, 20min aging showing partly faceted crystals. **(B)** magnified view of the marked region in **A**. The tip of the crystal is unfaceted. **(C)** Magnified view of the marked region in **B** showing apparent lattice fringes. Scale bar, 30 nm. **(D)** FFT analysis of **C** showing spacing of 1.6 nm.

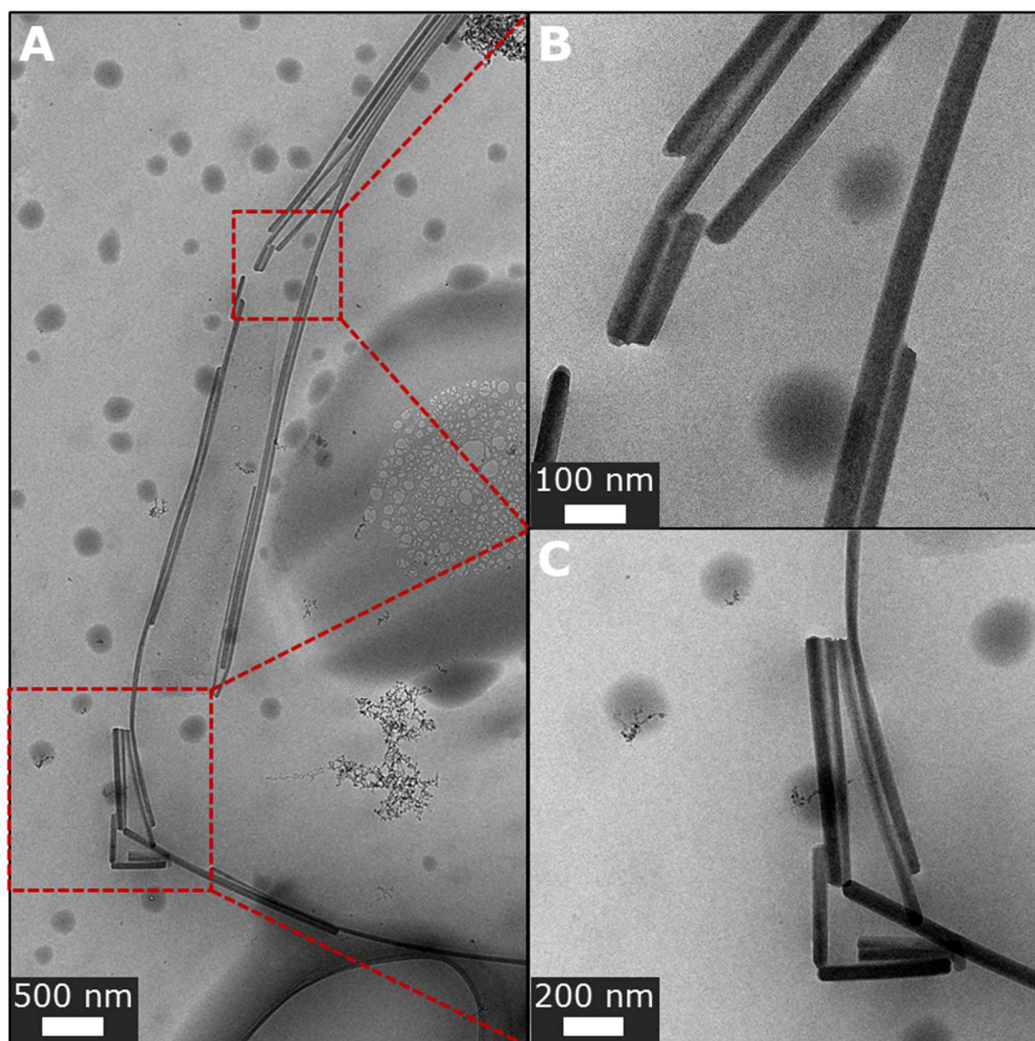


Figure S35. Cryo-TEM images of **2** grown in water/THF=7/3 (v/v) solution, 10^{-5} M, 3h aging. **(A)** Mature faceted crystals. **(B)-(C)** Magnified view of the corresponding marked regions in **A**.

References

- (1) Rosenne, S.; Grinvald, E.; Shirman, E.; Neeman, L.; Dutta, S.; Bar-Elli, O.; Ben-Zvi, R.; Oksenberg, E.; Milko, P.; Kalchenko, V.; Weissman, H.; Oron, D.; Rytchinski, B. Self-Assembled Organic Nanocrystals with Strong Nonlinear Optical Response. *Nano Lett.* **2015**, *15*, 7232–7237.
- (2) Demmig, S.; Langhals, H. Leichtlösliche, Lichtechte Perylen-Fluoreszenzfarbstoffe. *Chem. Ber.* **1988**, *121*, 225–230.
- (3) Juanhuix, J.; Gil-Ortiz, F.; Cuní, G.; Colldelram, C.; Nicolás, J.; Lidón, J.; Boter, E.; Ruget, C.; Ferrer, S.; Benach, J. Developments in Optics and Performance at BL13-XALOC, the Macromolecular Crystallography Beamline at the ALBA Synchrotron. *J. Synchrotron Radiat.* **2014**, *21*, 679–689.
- (4) Clays, K.; Persoons, A. Hyper-Rayleigh Scattering in Solution. *Phys. Rev. Lett.* **1991**, *66*, 2980–2983.
- (5) Macrae, C. F.; Edgington, P. R.; McCabe, P.; Pidcock, E.; Shields, G. P.; Taylor, R.; Towler, M.; van de Streek, J. Mercury : Visualization and Analysis of Crystal Structures. *J. Appl. Crystallogr.* **2006**, *39*, 453–457.